Textile Microwave Components in Substrate Integrated Waveguide Technology

Riccardo Moro, *Member, IEEE*, Sam Agneessens, *Student Member, IEEE*, Hendrik Rogier, *Senior Member, IEEE*, Arnaut Dierck, *Student Member, IEEE*, and Maurizio Bozzi, *Senior Member, IEEE*

***Abstract*—Although Substrate Integrated Waveguide (SIW) technology is well-established for the fabrication of microwave circuits on rigid printed circuit boards, and the first implementations of textile SIW antennas have recently appeared in literature, up to now, no complete set of SIW microwave components has been presented. Therefore, this paper describes the design, manufacturing, and testing of a new class of textile microwave components for wearable applications, implemented in SIW technology. After characterizing the adopted textile fabrics material in terms of electrical properties, it is shown that folded textile SIW components, such as interconnections, filters and antennas form excellent building blocks for wearable microwave circuits, given their low profile, flexibility and stable characteristics under bending and in proximity of the human body. Hence, they allow the full exploitation of the large area garments offered for the deployment of wearable electronics. Besides SIW interconnections, a folded textile SIW filter operating at 2.45 GHz is designed and tested. The filter combines excellent performance in the band of interest with good out-of-band rejection, even when accounting for the tolerances in the fabrication process. Finally, a folded SIW cavity-backed patch antenna is fabricated and experimentally verified in realistic operating conditions.**

***Index Terms*—Cavity-backed antenna, folded waveguide, substrate integrated waveguide, textile material, wearable systems.**

I. Introduction

THE development of novel applications for intelligent clothing and smart textiles is attracting more and more interest every year [1,2,3]. Specific application domains range from healthcare, over public safety, to military applications. In particular, wearable health monitoring is an attractive area for applications, given its very positive impact on the quality of life of the patients. Moreover, applications such as position tracking of rescue workers and communication with fire-fighters in critical conditions and harsh terrain motivate the research towards novel efficient wearable radio systems. Given its critical importance in wearable systems, the design of reliable wireless communication systems for wearable applications is a pivotal field of research.

Paper submitted on Feb. 19, 2014. This work was supported in part by the Italian Ministry of Education, University and Scientific Research under the project PRIN "GreTa" 2010WHY5PR.

R. Moro and M. Bozzi are with the University of Pavia, Department of Electrical, Computer and Biomedical Engineering, Pavia, Italy (e-mail: riccardo.moro@unipv.it, maurizio.bozzi@unipv.it). S. Agneessens, A. Dierck, and H. Rogier are with the Ghent University & iMinds, Department of Information Technology-IMEC, Ghent, Belgium (e-mail: sam.agneessens@intec.ugent.be, hendrik.rogier@ugent.be).

A textile integrated system performs its function while remaining conformal to the body shape and being comfortable to wear during deployment, without disturbing the movements of the user. Therefore, the development of passive components, active devices, and antennas, directly in textile material, is very challenging, since they must deliver high and stable performance in proximity of the human body, while maintaining the user's comfort. SIW technology is particularly suitable for implementation of wearable textile because of the simple manufacturing process, the possibility to fabricate conformal structures preserving the flexibility of the substrate and, last but not least, its capability to keep electromagnetic fields completely isolated from objects in its neighborhood, such as the human body. Moreover, SIW technology leverages the integration of different components into a single substrate, such as passive and active devices, antennas, etc. with a low-cost fabrication process. Therefore, low-profile multilayer SIW components can fully exploit the large area available in garments, by serving as building blocks of complete wearable microwave circuits. In addition, losses in SIW components may be minimized, thus increasing their efficiency [4, 5], even in proximity of the human body.

In terms of wearable textile microwave components, mainly antennas fabricated on textile materials have been proposed, combining robust electromagnetic performance with good wearer comfort [6]. In terms of topologies, mainly dipole antennas [7, 8, 9] and a variety of microstrip patch antennas operating in the industrial, scientific and medical (ISM) band (2.4–2.4835 GHz), [6, 10, 11, 12, 13] and in GPS-L1 band (1.56342-1.58742 GHz) [14, 15] were considered. Quite recently, the first SIW antenna [16] was introduced, followed by single band [17], dual band [18], and wideband [19] half-mode substrate integrated waveguide (HMSIW) textile antennas. These initial antenna designs prove the suitability of textile components in substrate integrated waveguide technology for body-worn systems.

In this paper, the implementation of a complete class of novel textile passive microwave components (interconnections, filters and antennas), realized in substrate integrated waveguide technology, is presented. Specifically, for the first time in literature, the folded SIW topology is applied to textile materials for the implementation of compact wearable microwave components, as this configuration achieves a size reduction without compromising the electromagnetic performance. Some specific guidelines are given to deal with fabrication tolerances and variations in material parameters typically encountered when designing components using textile materials. Furthermore, the

performance of the different components is validated in different adverse but realistic operation conditions, such as bending and body proximity.

In Sec. II, the basic issues in the design and fabrication of SIW on fabrics materials are discussed. In particular, dedicated framework is proposed, making use of broadband and narrowband algorithms, for the accurate electromagnetic characterization of fabric materials serving as substrates for SIW components. In Sec. III a single layer SIW interconnection is described, and in Sec. IV the designs of folded SIW components and their experimental characterization are reported in the light of the previous results. Finally a folded SIW cavity-backed patch antenna is presented.

II. Implementation Issues

A. Fabrication Process

The manufacturing process of textile-based SIW structures consists of the following steps: first of all, the conductive layers are cut from conductive fabric (specifically, electro textile), according to the layout of the design. Subsequently, these conductive layers are attached to the substrate by means of thermally activated adhesive sheets, paying particular attention to the alignment of different layers. Eventually, two or more substrate layers are glued together, to obtain a proper substrate thickness or to implement multilayer components. Finally, for the realization of metalized via holes, an eyelet press is used to fix the brass eyelets into the substrate at the correct locations. In fact, the use of eyelets provides a good ohmic contact between the two ground planes and preserves the flexibility of the structure (Fig. 1). Although the prototypes presented in the sequel were manufactured manually, an automated textile-based SIW fabrication process can easily be set up for mass production, by making use of industrial laminators, patterning systems, and a CNC automated eyelet punching machine.

In this work, a closed cell expanded rubber, usually adopted as a protective foam against impact, was chosen as a substrate for the fabrication of the SIW components. This specific material is light, flexible, flame retardant, and exhibits very good resistance against oils and solvents. For these reasons, it is commonly used in fire-fighters suits. Moreover, the foam is water-repellent and, hence, characterized by a low moisture regain, which ensures that its material properties at microwave frequencies will vary only little in various relative humidity conditions [20]. Therefore, wearable microwave components implemented using this substrate material will exhibit stable characteristics in realistic operation conditions. The 3.94 mm thick textile material adopted in this work is not produced for microwave applications and, therefore, the electrical characteristics of the foam are not perfectly known a-priori. In addition, they can vary slightly among different batches. In fact, the foam may exhibit small inhomogeneities of density and height, which can cause a moderate variability in the electrical parameters.

For the conductive layers, instead of copper sheets, a commercially available electro textile was adopted. The conductive Taffeta, a copper plated nylon fabric, is flexible and breathable, and exhibits a surface resistivity R_s=0.18 Ω/sq at 2.45 GHz, characterized by applying the technique described in [21].

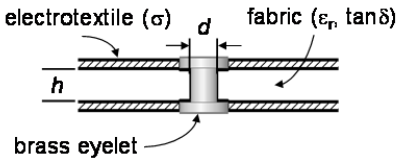

Fig. 1. Side view of SIW structure.

B. Design Challenges of SIW on Textile Fabrics

The design of textile microwave components presents challenges that are not usually faced when realizing circuits onto plastic or ceramic substrates, as typically encountered in microwave applications. In particular, specific issues related to the implementation of SIW structures on textile materials, such as compression and inhomogeneity of the fabric substrate, were also studied in [6, 16, 17].

For the implementation of SIW structures on textile substrates, the compression of the textile due to the via holes must be taken into account in the design. In fact, the techniques used for the metallization of the vias, such as embroidering a conductive yarn [17] or fixing the eyelets [16], cause compression of the substrate, and, consequently, a modification of the geometrical structure of the component. The compression may result in a variation of the cutoff frequency of SIW structures or a degradation of the performance in SIW components and circuits. Therefore, it is fundamental to consider these aspects in order to achieve a more realistic and accurate model of the SIW structure.

Another feature of fabric materials is their inhomogeneity, which is typical of flexible materials and that must be taken into account, especially when operating at high frequency. Moreover, traditionally, off-the-shelf fabrics are not completely characterized from the electromagnetic point of view, since they are not commonly adopted as microwave substrates. Yet, knowledge of the electrical properties of the textile materials is fundamental to correctly design the circuits. Consequently, an accurate characterization of the substrate over the frequency band of interest is mandatory. Several methods can be used to characterize the electrical properties of the material: among them, a very common approach is based on the measurements of interconnections with different lengths [22, 23]. The scattering parameters measurement of two interconnections with different lengths allows us to remove the influence of connectors and transitions by a de-embedding process, and to extract the electromagnetic properties from the complex propagation constant [22].

C. Dedicated Material Characterization Technique

In a first step, the electrical properties of the substrate in a broad frequency range were preliminarily determined by using a technique based on two microstrip lines with different length [21].

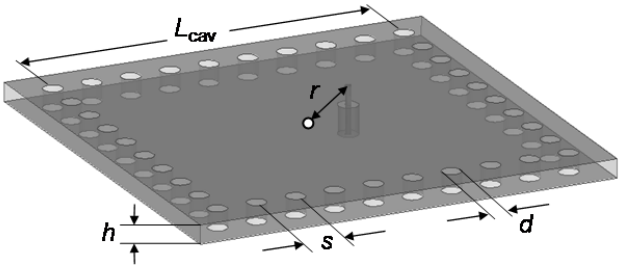

(*a*)

(*b*)

Fig. 2. Proposed SIW cavity: (*a*) structure (dimensions in mm: L_{cav}=74.7, *h*=3.94, *s*=8, *d*=4, *r*=21.2), (*b*) photograph of the prototype.

The use of this characterization technique yields the values of electric permittivity $\varepsilon_r = 1.575$ and the loss tangent $\tan\delta = 0.0238$, which represent a good starting point for the following steps in the characterization procedure.

Next, to verify the frequency dependence of the effective permittivity and the loss tangent of the foam, a dedicated material characterization technique was adopted. When deriving the effective electrical parameters of the substrate, it is essential to take into account some specific effects, related to the SIW implementation on textile materials, such as the compression of the substrate due to the pressure of the eyelets. This method consists of analyzing the resonance frequencies and the quality factors of a square SIW cavity. The substrate is a single-layer textile with a thickness of h=3.94 mm. The lateral walls of the cavity were implemented by means of eyelets with a diameter of d=4 mm and a total height of 6 mm (consisting of a metal cylinder of approximately 4 mm and two flanges). The height of eyelets was selected to guarantee the metallization of the via holes and a good connection between the bottom and top metal layers of the cavity. Based on the previous knowledge of the electrical characteristics of the substrate and of the conductive Taffeta, the dimensions of the structure were selected in such a way that the resonant frequency of the fundamental (quasi TM_{110}) mode was approximately 2.45 GHz, corresponding to the center frequency of the 2.4 GHz ISM band. The cavity is excited by a coaxial line through a surface-mount adjustable (SMA) connector (Fig. 2). The prototype of the SIW cavity is shown in Fig. 2*b*.

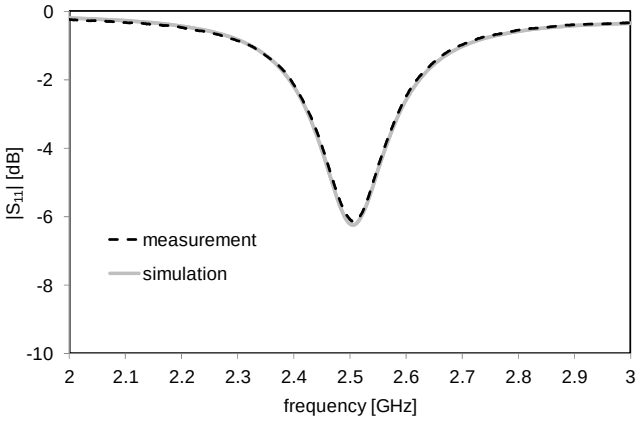

Fig. 3. Measured and simulated input matching of the SIW cavity.

The measurement of the cavity provided a resonance frequency of the fundamental mode at 2.506 GHz (Fig. 3, black line). Consequently, the first step to determine the electrical properties of the substrate was the estimation of the permittivity by a parametric analysis; by setting the value of $\varepsilon_r = 1.45$ in the simulation setup, a perfect overlap between measured and simulated resonance frequency was achieved.

As a second step, to identify the losses of the substrate, the quality factor related to the dielectric losses was calculated. The quality factor Q_D of the cavity can easily be derived from the unloaded quality factor (Q_U) and the quality factor related to the conductor losses (Q_C) [22]. Moreover, also the radiation losses should be considered. However, since the design rule $s = 2d$ is respected [4], this type of loss can be neglected. By adopting the equivalent waveguide concept [5], the quality factor related to the conductor losses can be computed analytically: the equivalent conventional rectangular cavity was studied considering the conductivity of Taffeta for the top and bottom layers, and the conductivity of brass for the lateral walls. The calculated value of Q_C is 207. In order to confirm this result, a numerical simulation of the SIW structure was performed by using the electromagnetic solver Ansys HFSS. The value computed by HFSS was 211, which validates the result achieved with the analytical method.

Conversely, the unloaded quality factor Q_U can be estimated directly from the measured input matching of the fabricated SIW cavity with the method described in [24]. First of all, the coupling coefficient *k* is calculated by

$$k = \frac{1 - 10^{-S_{11}^{min}/20}}{1 + 10^{-S_{11}^{min}/20}} \qquad (1)$$

where S_{11}^{min} is the minimum value of the input matching $|S_{11}|$ expressed in dB. In order to make a correct evaluation, the feeding pin was not located near the center of the cavity, as at that point, S_{11}^{min} is more sensitive to positioning errors. The distance $r = 21.2$ mm (Fig. 2(*a*)) between the coaxial line and the center of the cavity permits a more accurate estimation of S_{11}^{min}. Afterwards, the value of the input matching at the frequency where the phase of S_{11} is 45° (S_{11}^{Φ}) was determined by using the next formula [24].

$$S_{11}^{\Phi} = 10\log\frac{1+10^{-S_{11}^{\min}/10}}{2} \quad (2)$$

Finally, Q_L is computed by

$$Q_L = \frac{f_L}{f_2 - f_1} \quad (3)$$

where f_L is the resonance frequency of the fundamental cavity mode, whereas f_1 and f_2 are the frequencies corresponding to $|S_{11}|=|S_{11}^{\Phi}|$. The quality factor Q_U of the cavity is estimated starting from the Q_L and the coupling coefficient k, using

$$Q_U = Q_L(1+k) \quad (4)$$

From these analyses, it results that $Q_U = 46$ and consequently, that $Q_D = 59.5$. Once Q_D is obtained, $\tan\delta$ can be calculated as

$$\tan\delta = \frac{1}{Q_D} \quad (5)$$

Taking into account the accuracy of the estimation of the quality factor (in order of 10%), the value of loss tangent derived in this way is 0.017.

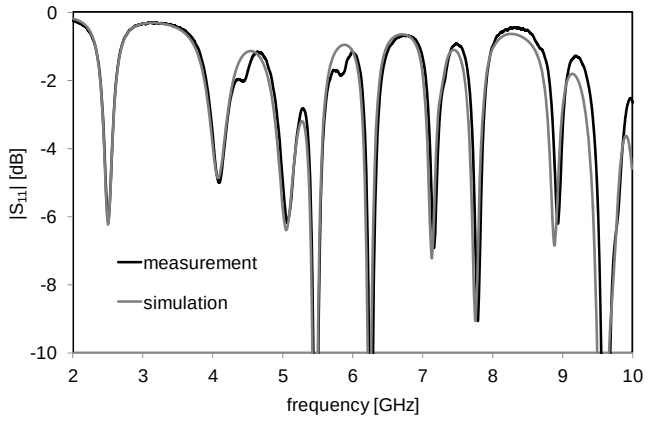

(*a*)

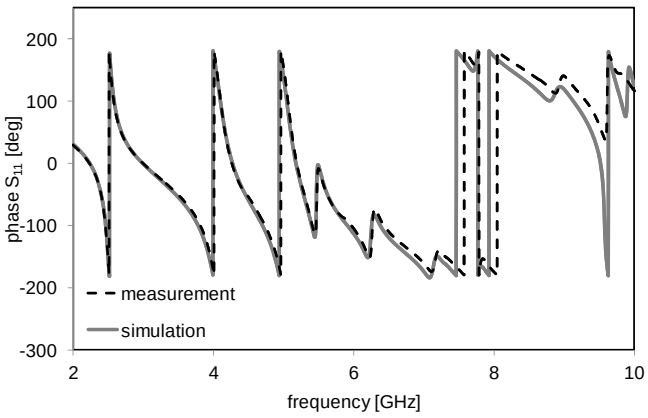

(*b*)

Fig. 4. Measured and simulated input matching of the SIW cavity: (*a*) magnitude, (*b*) phase.

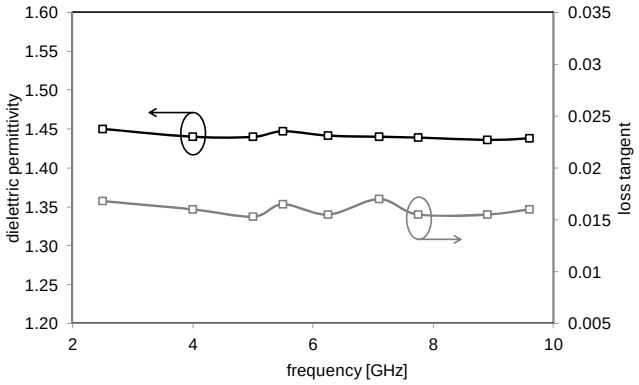

Fig. 5. Estimated dielectric permittivity and loss tangent of the textile material.

After completing this material characterization technique, the cavity was re-simulated with the updated values of relative dielectric permittivity ε_r=1.45 and loss tangent $\tan\delta$=0.017.

As shown in Fig. 3, the frequency response of the reflection coefficient, simulated by using the updated electrical parameters, perfectly overlaps with the measured result. In addition, the measured and simulated input matching of the SIW cavity were compared over a broader frequency range, namely from 2 to 10 GHz (Fig. 4).

The simulated data shown in Fig. 3 and in Fig. 4 were obtained by taking into account the SMA connectors, which are not included in the calibration of the measurement setup. In this way, the measured and simulated data can be compared since the reference plane is the same, and any error in the phase of the input matching is avoided. A good agreement, for both magnitude and phase of S_{11} can be observed in Fig. 4. Yet, beyond 8 GHz, a slight shift of the resonances and incorrect levels of the local maxima of magnitude as well as a discrepancy in the phase can be noticed.

Further analyses were performed to evaluate the electrical characteristics of the textile material as a function of frequency. According to the method presented, the estimation of the dielectric permittivity and loss tangent can be done only at the resonant frequencies of the cavity. For each resonance, the electrical parameters were extracted with the method described above, and the curves of the estimated values of ε_r and $\tan\delta$ were estimated (Fig. 5). The graph shows that the electrical parameters of the substrate are quite constant over a wide bandwidth and the estimated values ($\varepsilon_r = 1.45$ and $\tan\delta = 0.017$) are a good approximation even for relatively high frequencies.

III. Single-Layer SIW Textile Interconnection

After evaluating the electrical characteristics of the substrate, an SIW interconnection on textile was designed. Since the band of interest is the ISM band around 2.45 GHz, the interconnection was designed with a cutoff frequency of the fundamental mode $f_0 = 1.62$ GHz. This performance can be obtained by properly selecting the geometrical dimensions of the SIW structure (Fig. 6*a*) [4].

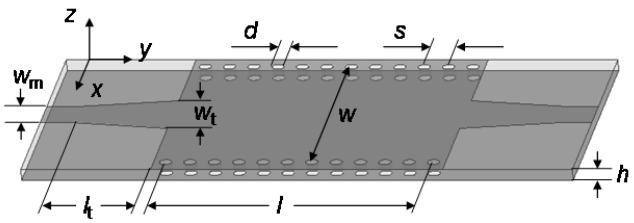

(*a*)

(*b*)

Fig. 6. Proposed SIW interconnection: (*a*) structure (dimensions in mm: l_t=32.7, w_t=23, w_m=13, h=3.94, s=8, d=4, w=79, l=96), (*b*) photograph.

In particular, the width of the SIW is w = 79 mm, the diameter of metal vias is d = 4 mm and their longitudinal spacing is s = 8 mm. The adopted substrate is a single foam layer, with a thickness of 3.94 mm. In order to characterize the component by a network analyzer, the transitions from 50-Ω microstrip line to SIW were included in the design of the interconnection (l_t = 32.7 mm, w_t = 23 mm, w_m = 13 mm). A prototype of the SIW interconnection with a length l = 96 mm is shown in Fig. 6*b*.

Fig. 7*a* shows the simulated and measured magnitude of scattering parameters of the SIW interconnection. The measured cutoff frequency of the (quasi) TE_{10} mode is 1.65 GHz and the insertion loss at 2.45 GHz is 2 dB. Both $|S_{11}|$ and $|S_{22}|$ exhibit a good agreement between simulated and measured data, demonstrating the precision of the substrate material characterization and the reliability of the fabrication process. A good agreement is also shown in Fig. 7*b*, in which the measured and simulated phases of S_{21} are compared. In this case, as for the cavity, the effect of the connectors that terminate the SIW interconnection is taken into account in the simulation. The goodness of the estimation of the electrical properties of the substrate is demonstrated by the perfect overlapping of the two curves.

As already mentioned, thanks to the flexibility of the material, the use of textile as substrate for microwave systems opens new perspectives in the applications, which include the employment of conformal structures. In this condition the effect of bending has to be studied. Therefore, the S-parameters of the SIW interconnection for a bending radius of 50 mm were measured. As shown in Fig. 8, the effect of the deformation can be considered negligible since only small changes in the cut-off frequency of the waveguide can be noticed.

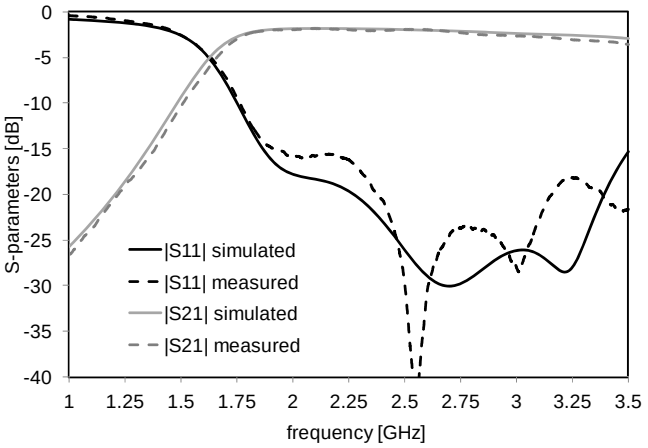

(*a*)

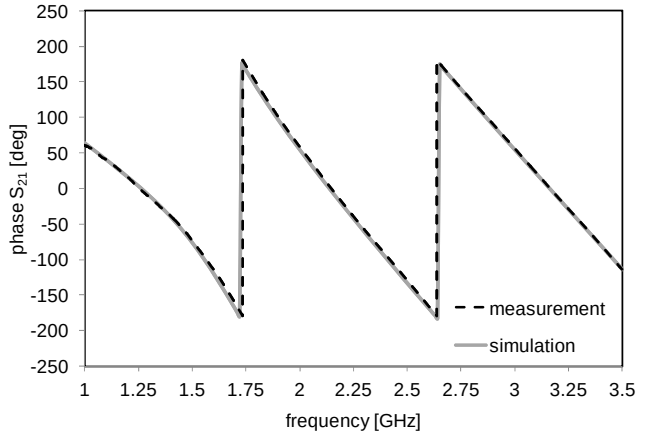

(*b*)

Fig. 7. Measured and simulated scattering parameters of the SIW interconnection: (*a*) magnitude, (*b*) phase.

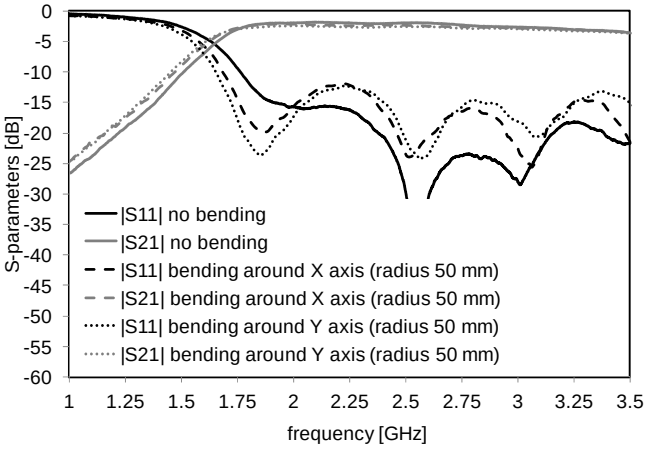

Fig. 8. Measured scattering parameters of the SIW interconnection.

In fact, the average value of the $|S_{21}|$ in the transmission band remains at -2 dB and the reflection coefficient of the component is still smaller than -10 dB.

IV. Folded SIW Textile Components

The implementation of substrate integrated folded waveguide (SIFW) components was subsequently investigated. The SIFW structure consists of a standard SIW folded around a metal septum. The SIFW configuration was proposed for the first time in [25] and permits to achieve a considerable reduction in the footprint of the components, while keeping comparable performance as a standard SIW. In fact, the width of the waveguide can be decreased by more than 50%, at the cost of an increase of a factor two in thickness.

For the implementation on textile, the structure consists of two stacked substrate layers with the upper and lower faces metalized, a conductive sheet glued in between them, and two rows of eyelets as lateral walls. A gap is defined between one side of the waveguide and the center conductor, as shown in Fig. 9*a*.

In the design of the SIFW interconnection, the gap *g* plays a fundamental role in the performance of the waveguide. In fact, once the width *w* and the height *h* of the SIFW are fixed, the dimension *g* significantly affects the cutoff frequency of the fundamental mode, while the cutoff frequency of the second (quasi TE_{20}) mode remains unchanged. A larger gap produces an upward shift of the cutoff frequency of the (quasi) TE_{10} mode. This behavior can be explained by a circuit-oriented approach: the variation of the gap width causes a variation of the capacitance per unit length of the waveguide.

The SIFW configuration proves particularly suitable for the implementation of textile components, because multilayer components are perfectly feasible on textile and, at the same time, the reduction in dimension enables the integration of complete on-body systems (including interconnections, passive components, and antennas).

A. SIFW Interconnection

The proposed SIFW interconnection was designed to exhibit the same cutoff frequency of the fundamental mode as the SIW interconnection presented in Section III (f_0=1.62 GHz). In the design, two textile layers with thickness h=3.94 mm were adopted. The width of the waveguide resulted to be w = 41.2 mm, which corresponds to a reduction of 47.8% with respect to the standard SIW interconnection. Furthermore, the dimension of the gap *g* was set to 4 mm. This value was chosen conservatively by taking into account the potential inaccuracy of the fabrication process. In fact, even though this value does not permit to minimize the width of the waveguide, it avoids any undesired contact between the central metal sheet and the side wall made of eyelets. Finally, a 50 Ω stripline-to-SIFW was designed for maximum operation bandwidth (l_t=28.7 mm, w_t=19.6 mm, w_m=8.5 mm). In Fig. 9*b* a photograph of the substrate integrated folded waveguide is shown. The component and the transitions are completely shielded by two sheets of conductive Taffeta. Fig. 10 shows the simulated and measured scattering parameters of the SIFW interconnection with a length l = 96 mm.

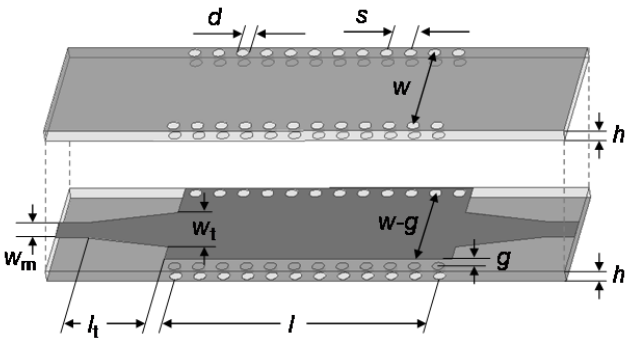

(*a*)

(*b*)

Fig. 9. Proposed SIFW interconnection: (*a*) structure (dimensions in mm: l_t=28.7, w_t=19.6, w_m=8.5, h=3.94, s=8, d=4, g=4, w=41.2, l=96), (*b*) photograph.

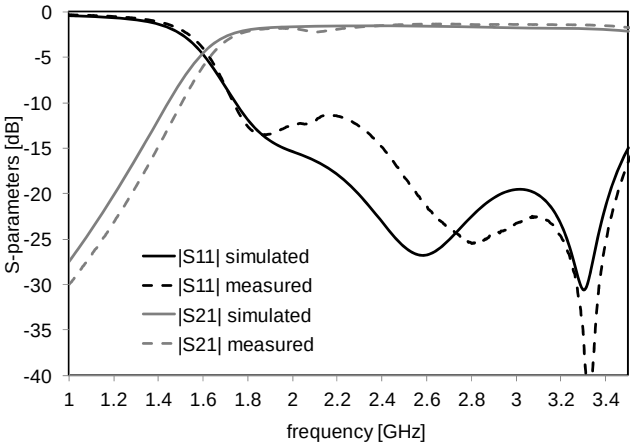

Fig. 10. Simulated and measured scattering parameters of the SIFW interconnection.

The insertion loss curves are in good agreement in the operation bandwidth of the SIFW, whereas the cutoff frequency has slightly shifted upward by 45 MHz. The reason of this mismatch is attributed to the misalignment of the central conductive sheet. In fact, a small error of the value *g* in the prototype can explain the frequency shift. The insertion loss of the SIFW interconnection is 1.49 dB at 2.45 GHz, a value that is smaller than the insertion loss of the SIW interconnection in Sec. III.

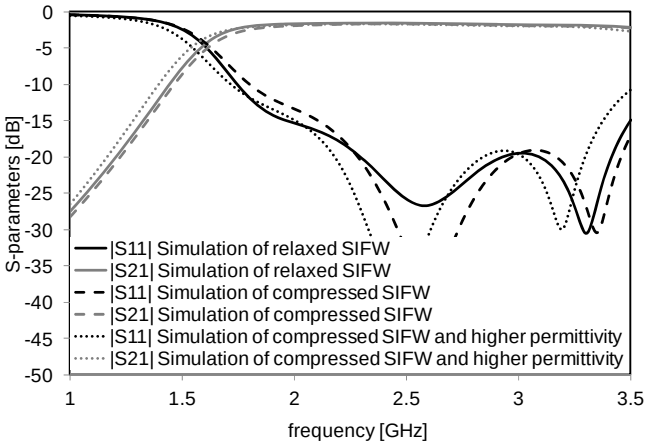

Fig. 11. Simulated scattering parameters of the SIFW interconnection exposed to mechanical stress.

The smaller insertion loss can be explained by the different transitions to planar interconnections: in case of the SIFW, a stripline is adopted, which is completely shielded and does not exhibit any radiation losses. On the contrary, the microstrip-to-SIW transition applied in the design discussed in Sec. III suffers from small radiation losses.

In real-life applications, the textile components are exposed to mechanical stress, which can deteriorate the performance of the components. For this reason the effect of compression onto the folded SIW interconnection was investigated. The protective foam applied as substrate exhibits a compression set of 30% [6], which means of after compressing the substrate for 72 hours, the material only regains 70% of its original height. Therefore, two different simulations of compression were performed. In the first setup, the thickness of each layer of the interconnection was reduced to 2.76 mm instead of the original 3.94 mm (30% of reduction). The results of Fig. 11 show that only a small upward shift of the cut-off frequency is obtained: the decrease of the thickness influences the electric field in the gap area and causes a reduction of the total width of the interconnection. However, the resulting effect is modest since, except for the gap portion, the field configuration of the fundamental mode of the SIFW interconnection is not affected by the change in the thickness of the waveguide.

Besides the reduction in height, compression of textile fabrics and foams will typically also cause in increase in material permittivity, as experimentally verified in [25]. Hence, a second analysis was performed considering both a 30% reduction in thickness of the structure and a 10% increase of the dielectric permittivity [6]. The effect on the frequency response is a shift towards lower frequencies of the cut-off frequency of the quasi-TE_{10} mode (Fig. 11). The variation due to the change of ε_r is more significant than the compression phenomenon, since it considerably affects the electromagnetic behavior of the SIFW interconnection.

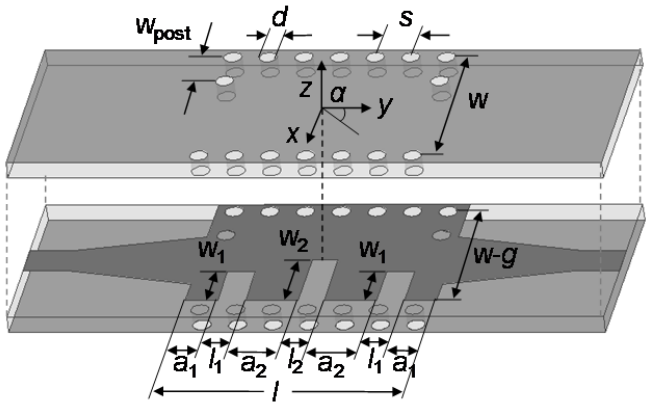

Fig. 12. Proposed topology of the SIFW filter (dimensions in mm: w=41.2, g=4, d=4, s=8. l=56.3, w_{post}=9.9, l_1=6.3, l_2=5.9, w_1=12, w_2=17, a_1=7.2, a_2=11.7).

B. SIFW Bandpass Filter

A two-pole SIFW bandpass filter was designed to operate in the frequency band centered at 2.45 GHz. Several typologies of filters are suitable for implementation in folded integrated waveguide. Among others, the most common are the standard inductive iris filter [5], the filter with H-plane septa [26, 27], and the H-plane filter with transversal slots [27].

The proposed filter on the textile substrate is based on the last topology. This topology was selected because it is compact and it exhibits a better out-of-band rejection than the other classes of filters. The structure consists of an SIFW with three slots cut out in the central conductive sheet. Moreover, two metalized posts at the two ends of the filter were added as shown in Fig. 12. A 50 Ω stripline-to-SIFW transition was designed for testing the component.

The filter was fabricated and experimentally verified with a network analyzer. The measured results are in good agreement with simulated data (Fig. 13*a*). The 3 dB bandwidth of the filter is 725 MHz and the insertion loss is 2.3 dB at 2.45 GHz.

The frequency response of $|S_{11}|$ exhibits two poles, which correspond to even and odd resonant modes of the cavity defined by the two posts (as shown in Fig. 13*b*). The desired frequency response in the band of interest was achieved through the analysis of the mode spectrum of the SIFW cavity including the insets. Moreover, the dimensions of the transversal slots were optimized to obtain a very good selectivity above the transmission band. A good out of band rejection is achieved thanks to the symmetry of the filter (including the feeding lines) with respect the metal septum; in this condition the cavity modes, which satisfy the electric wall condition on the plane of symmetry, are not excited. Furthermore, the metalized holes near the transitions improve the frequency response in the lower frequency range. In fact, the addition of the posts permits to improve the selectivity of the filter and the out of band rejection at low frequencies.

This configuration permits to significantly reduce the length of the filter. Therefore, by limiting the propagation path of the electromagnetic field in the lossy textile substrate, the insertion loss in the operation band decreases.

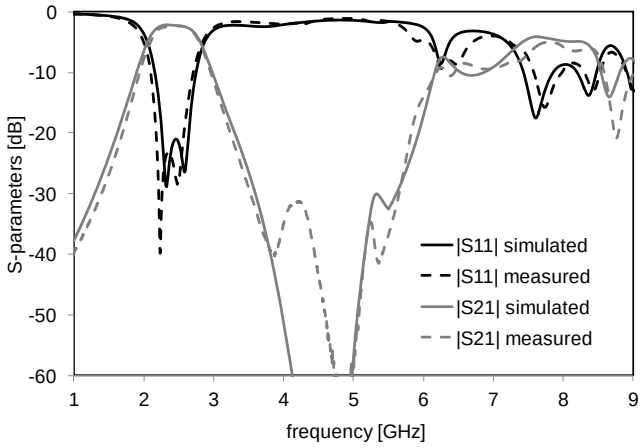

(*a*)

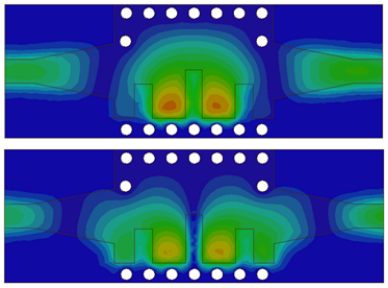

(*b*)

Fig. 13. Textile SIFW filter: (*a*) simulated and measured scattering parameters of the SIFW filter; (*b*) plot of the magnitude of the electric field at 2.33 GHz (left) and 2.59 GHz (right).

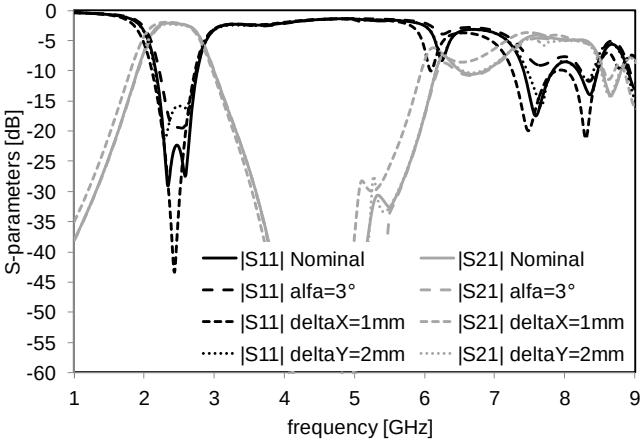

Fig. 14. Simulated scattering parameters of the SIFW filter exposed to fabrication inaccuracies.

To verify the robustness of the filter design, a set of parametric analyses were performed. In particular, the inaccuracies due to the fabrication process were simulated to investigate the level of degradation introduced in the performance of the SIFW filter. Three different error contributions in position of the central metal layer were analyzed: a shift along X axis, a shift along Y axis, and a rotation with respect the centre of the structure.

Fig. 14 shows the frequency response of the filter for three different configurations. The obtained results show that the behavior of the SIFW filter in the frequency band of interest is not dramatically altered even if the deterioration is not negligible. Nevertheless the out of band rejection remains good over a broad bandwidth. It is important to underline that the simulations shown in Fig. 14 correspond to inaccuracies in the fabrication process that are overstated even if the prototype is constructed manually.

V. Folded SIW Cavity-Backed Patch Antenna

Besides passive components such as interconnections and filters, a folded SIW cavity-backed patch antenna was designed and implemented on textile. In fact, for wearable applications implementing wireless communication, the antenna is one of the most important components of the system, as it should guarantee good radiation performance as well as unobtrusive and comfortable integration in a garment. A fundamental characteristic of the antenna topology should be its small size, because it enables easier integration into suits. For this reason SIFW technology was adopted, to reduce the dimensions of the antenna by realizing a multilayer structure.

The proposed antenna topology consists of a folded SIW cavity with a square ring aperture cut out in the top metal layer, thus forming a radiating patch with side L_2 (Fig. 15*a*). In order to obtain the folded SIW cavity, two textile layers with the same thickness of 3.94 mm were stacked and an inner metal patch with side L_1 was glued in between them. A metal via, implemented by a rivet with a diameter of 2 mm, was placed at the centre of the cavity to connect the bottom ground plane and the lower metal patch. The via holes that define the lateral walls of the cavity were properly spaced to avoid radiation leakage ($s=2d_2$). The side length L_1 of the inner patch was chosen in order to both minimize the dimensions of the cavity and prevent high conductor losses, which could arise in when a small gap between the metal patch and the side walls of the SIW cavity is used. The dimensions of the square ring slot cut out in the top metal sheet were selected to maximize the radiation efficiency and to broaden the operating bandwidth of the antenna.

The antenna is fed from the back side by a coaxial probe. The position of the feeding pin was chosen for optimal coupling with the fundamental mode of the metal patch. A good input matching can be obtained with the feeding point located on the diagonal of the patch, 11.3 mm away from the centre of the cavity. The position of the feed permits to achieve broadside radiation with the electric field linearly polarized along the diagonal of the cavity.

A prototype of the antenna was fabricated, and some photographs are shown in Fig. 15*b*,*c*.

Finally, the antenna was measured in stand-alone conditions to evaluate its electromagnetic performance. The simulated and measured input matching characteristics of the antenna are shown in Fig. 16*a*. From the measurement it is clear that the specification for the 2.4 GHz ISM band is fulfilled since the reflection coefficient is smaller than -10 dB over a bandwidth of 130 MHz around the 2.45 GHz, with a maximum input matching at the frequency of 2.43 GHz.

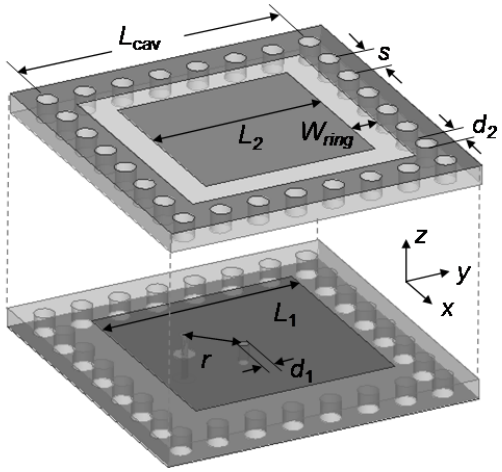

(*a*)

(*b*) (*c*)

Fig. 15. Folded SIW cavity-backed patch antenna: (*a*) structure (dimensions in mm: L_{cav}=54.1, L_2=35, W_{ring}=5.5, L_1=41.2, d_1=2, d_2=4, s =8, r =11.3); (*b*) photograph of the feed side; (*c*) photograph of the radiating side.

Additionally, the influence of mechanical bending was experimentally evaluated: the antenna was bent around a cylinder with radius of 50 mm. Both bending around the X axis and around the Y axis were considered. The variation of the input matching due to bending is negligible, as shown in Fig. 16*b*. This result proves that the antenna characteristics will remain stable both when the antenna is deployed on persons of different body morphology and when the antenna bends due to movements of the wearer. A more detailed statistical analysis may be applied to study bending effects following the procedure outlined in [28].

Moreover, the effect of the compression was investigated. The same phenomena already studied for the SIFW interconnection were analyzed, but the results achieved are very different. In fact, as shown in Fig. 16*c*, the effect of compression is much more significant than in the previous analysis. It causes a shift to higher frequency in the reflection coefficient of the antenna which, when the dielectric permittivity is adjusted, returns to satisfy the ISM band specifications. For the folded SIW cavity-backed patch antenna, the effect of compression on the reflection coefficient is balanced by the increase in permittivity directly caused by the mechanical stress.

Furthermore, the radiation pattern of the antenna was measured in anechoic chamber. In particular, taking into account the polarization of the antenna, the radiation pattern

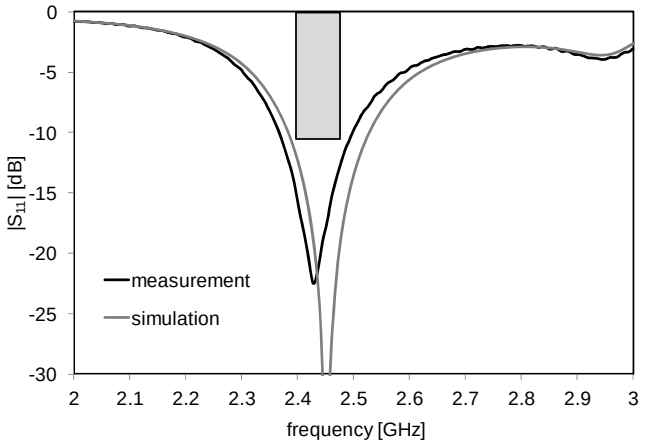

(*a*)

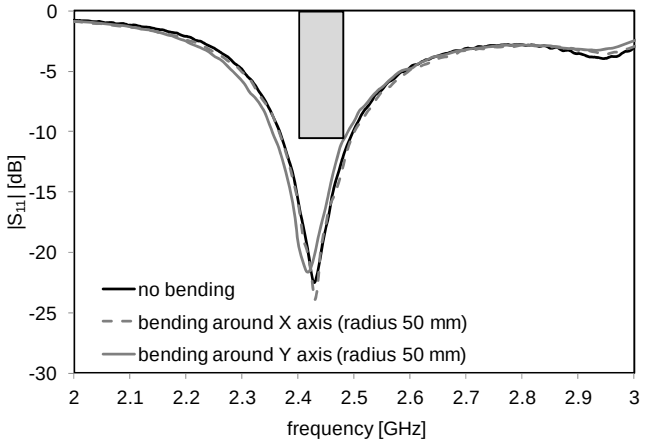

(*b*)

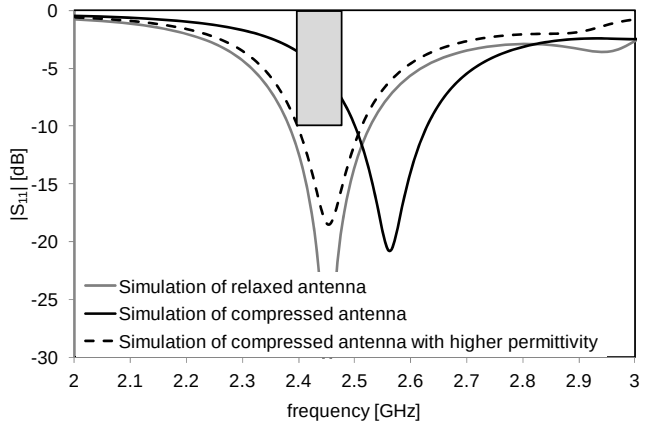

(*c*)

Fig. 16. Input matching of the folded SIW cavity-backed antenna: (*a*) simulation and measurement under ideal conditions; (*b*) measurements with effect of bending; (*c*) simulations with mechanical stress.

on planes $\Phi = 45°$ and $\Phi = 135°$ was measured at the frequency of 2.45 GHz. Fig. 17 shows the comparison between simulation and measurement, which are in very good agreement. The antenna provides an efficiency of 74%, with a maximum gain of 5.93 dBi at boresight direction, which is consistent with the simulated value (5.9 dBi). The front-to-back ratio of the antenna is approximately 18 dB.

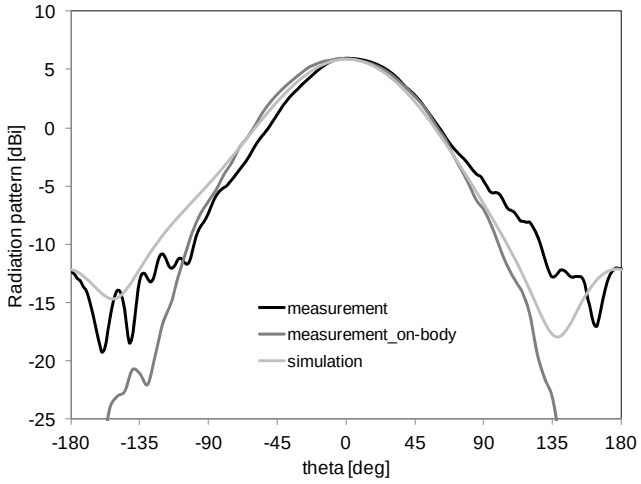

(*a*)

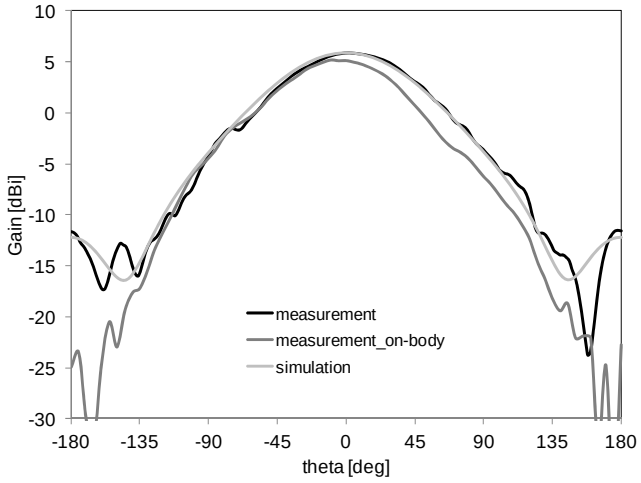

(*b*)

Fig. 17. Simulated and measured radiation patterns of the folded SIW cavity-backed antenna: (*a*) in the plane $\Phi = 45°$; (*b*) in the plane $\Phi = 135°$.

Finally, the antenna was integrated into a human body-worn jacket, and its electrical characteristics were measured. The effect on the reflection coefficient is negligible and the radiation patterns on the two planes of interest remain very similar to the measurements in stand-alone condition (Fig. 17). These measurements confirm the suitability of SIW components for on-body applications. In fact, by adopting this technology, we achieved a low influence of human body on the performance of the antenna and an high front-to-back ratio which is fundamental to reduce the Specific Absorption Rate (SAR). Furthermore, the folded SIW antenna provides a small footprint with respect to other textile antenna: a 43% of reduction with respect to [16] and a 80% of reduction with respect to [13] where the design includes an EBG structure to improve the front-to-back ratio and reduce the radiation toward the body.

VI. Conclusion

The design of several SIW components and antennas, realized entirely in textile materials, has been presented. The values of the electrical parameters employed in the designs were extracted by means of a dedicated characterization technique, based on the measurement of a SIW cavity. Interconnections, as well as a band-pass filter and a cavity-backed antenna, were realized in order to investigate the use of the folded substrate integrated waveguide technology (SIFW) for wearable electronics. The fabricated prototypes are light-weight, flexible, and very compact. They exhibit good electromagnetic performance, in comparison to implementations on more conventional microwave materials. These characteristics make the components suitable for a complete integration in smart textiles. Moreover, our measurement results, together with those obtained in [16], indicate that high robustness against bending is obtained, thus making textile SIW circuits well-suited for on-body use.

References

[1] J. Lilja, V. Pynttari, T. Kaija, R. Makinen, E. Halonen, H. Sillanpaa, J. Heikkinen, M. Mantysalo, P. Salonen and P. de Maagt, "Body-Worn Antennas Making a Splash: Lifejacket-Integrated Antennas for Global Search and Rescue Satellite System," *Antennas and Propagation Magazine, IEEE*, vol. 55, no. 2, pp. 324-341, 2013.

[2] S. Agneessens, P. V. Torre, F. Declercq, B. Spinnewyn, G. J. Stockman, H. Rogier and D. Vande Ginste, "Design of a Wearable, Low-Cost, Through-Wall Doppler Radar System," *International Journal of Antennas and Propagation*, vol. 2012.

[3] S. Agneessens, P. Van Torre, E. Tanghe, G. Vermeeren, G., W. Joseph and H. Rogier, "On-Body Wearable Repeater as a Data Link Relay for In-Body Wireless Implants," *Antennas and Wireless Propagation Letters, IEEE* , vol.11, no., pp.1714-1717, 2012.

[4] M. Bozzi, A. Georgiadis, and K. Wu, "Review of Substrate Integrated Waveguide (SIW) Circuits and Antennas," *IET Microwaves, Antennas and Propagation*, Vol. 5, No. 8, pp. 909–920, June 2011.

[5] R. Garg, I. Bahl, M. Bozzi, *Microstrip Lines and Slotlines*, 3rd ed. Norwood, MA, USA: Artech House, 2013.

[6] C. Hertleer, H. Rogier, L. Vallozzi, and L. Van Langenhove: "A Textile Antenna for Off-Body Communication Integrated Into Protective Clothing for Firefighters," *IEEE Transactions on Antennas and Propagation*, Vol. 57, No. 4, pp. 919-925, April 2009.

[7] D. Psychoudakis, C.-C. Chen, and J. Volakis, "Wearable UHF antenna for squad area networks (SAN)," *IEEE Antennas and Propagation Society International Symposium*, pp. 1–4, July 2008.

[8] L. Ukkonen, L. Sydanheimo, and Y. Rahmat-Samii, "Sewed textile RFID tag and sensor antennas for on-body use," *6th European Conf. Antennas and Propagation (EUCAP)*, pp. 3450 –3454, Mar. 2012.

[9] T. Kaufmann, I.-M. Fumeaux, and C. Fumeaux, "Comparison of fabric and embroidered dipole antennas," in *Proc. 7th EuCAP*, Gothenburg, Sweden, Apr. 2013.

[10] I. Locher, M. Klemm, T. Kirstein, and G. Troster, "Design and characterization of purely textile patch antennas," *IEEE Transactions on Advanced Packaging*, Vol. 29, No. 4, pp. 777–788, Nov. 2006.

[11] M. Scarpello, D. Vande Ginste, H. Rogier, "Design of a low-cost steerable textile array operating in varying relative humidity conditions," *Microwave Optical Technology Letters*, Vol. 54, No. 1, pp. 40-44, 2012.

[12] J.G. Santas, A. Alomainy, H. Yang, "Textile Antennas for On-Body Communications: Techniques and Properties," in *Proc. 2nd EuCAP*, Edimburgh, Scotland, Nov. 2007.

[13] S. Z. Zhu and R. Langley, "Dual-band wearable textile antenna on an EBG substrate," *IEEE Trans. Antennas Propag.*, vol. 57, no. 4, pp. 926–935, Apr. 2009.

[14] L. Vallozzi, W. Vandendriessche, H. Rogier, C. Hertleer, and M. L. Scarpello, "Wearable textile GPS antenna for integration in protective garments," in *Proc. 4th Eur. Conf. Antennas Propag*, pp. 1–4, 2010.

[15] P. Salonen, Y. Rahmat-Samii, M. Schaffrath, and M. Kivikoski, "Effect of textile materials on wearable antenna performance: a case study of GPS antennas," *IEEE Antennas and Propagation Society International Symposium*, Vol. 1, pp. 459–462, June 2004.

[16] R. Moro, S. Agneessens, H. Rogier, and M. Bozzi, "Wearable Textile Antenna in Substrate Integrated Waveguide Technology," *IET Electronics Letters*, Vol. 48, No. 16, pp. 985–987, August 2, 2012.

[17] T. Kaufmann and C. Fumeaux, "Wearable textile half-mode substrate integrated cavity antenna using embroidered vias," *IEEE Antennas and Wireless Propagation Letters*, Vol. 12, pp. 805–808, 2013.

[18] S. Agneessens, and H. Rogier, "Compact Half Diamond Textile HMSIW On-Body Antenna", *IEEE Trans. Antennas Propag,* vol.62, in press.

[19] S. Lemey, F. Declercq, and H. Rogier, "Dual-Band Substrate Integrated Waveguide Textile Antenna With Integrated Solar Harvester," *Antennas and Wireless Propagation Letters, IEEE* , vol.13, no., pp.269,272, 2014

[20] C. Hertleer, A. Van Laere, H. Rogier, L. Van Langenhove, "Influence of Relative Humidity on Textile Antenna Performance.," Textile Research Journal (IF 1.102, ranking 3/21, Q1, 24 citations), vol. 80, no. 2, pp. 177–183, Jan. 2010.

[21] F. Declercq, I. Couckuyt, H. Rogier, and Tom Dhaene, "Environmental High Frequency Characterization of Fabrics based on a Novel Surrogate Modelling Antenna Technique", *IEEE Trans. on Antennas Propag.*, Vol. 61, No. 10, pp. 5200–5213, Oct. 2013.

[22] F. Declercq, H. Rogier, and C. Hertleer, "Permittivity and loss tangent characterization for garment antennas based on a new matrix-pencil two-line method," *IEEE Transaction of Antennas and Propagation*, Vol. 56, No. 8, pp. 2548–2554, Aug. 2008.

[23] M. D. Janezic, J.A. Jargon, "Complex permittivity determination from propagation constant measurements," *IEEE Microwave and Guided Wave Letters*, Vol. 9, No. 2, pp. 76–78, Feb. 1999.

[24] R. J. Cameron, C. M. Kudsia, R. R. Mansour, *Microwave resonator in Microwave Filters for Communication Systems*, 1st ed., Ed. Hoboken, New Jersey: John Wiley & Sons, pp.427-428, 2007.

[25] F. Boeykens, L. Vallozzi, and H. Rogier, "Cylindrical bending of deformable textile rectangular-patch antennas," International Journal of Antennas and Propagation, Article ID 170420, 11 pages, doi:10.1155/2012/170420, 2012.

[26] N. Grigoropoulos, B. Sanz-Izquierdo, P.R. Young, "Substrate integrated folded waveguides (SIFW) and filters," *IEEE Microwave and Wireless Components Letters*, Vol. 15, No. 12, pp. 829-831, Feb. 2005.

[27] Z. Wang, D. Shen, R. Xu, B. Yan, W. Lin, Y. Guo, X. Xie, "Partial H-plane bandpass filters based on substrate integrated folded waveguide (SIFW) ," *Proc. of Asia Pacific Microwave Conference*, Dec. 2009.

[28] F. Boeykens, H. Rogier, and L. Vallozzi, "An efficient technique based on polynomial chaos to model the uncertainty in the resonance frequency of textile antennas due to bending", IEEE Trans. on Antennas Propag., vol. 62 , no. 3, pp. 1253–1260, Mar. 2014.